ASEAN
Journal of Scientific and Technological Reports
Online ISSN:2773-8752

Research article

Environmental Impact Assessment of Onshore Wind Power Plants: A Case Study of a 50 MW Wind Power Plant in Northeastern Thailand

Sunisa Kongprasit[1], Somphol Chiwamongkhonkarn[2], Fida Ali[3], Pongsak Makhampom[4], Yves Gagnon[5] and Jompob Waewsak[6*]

[1] Faculty of Science and Digital Innovation, Thaksin University, Phatthalung, 93210, Thailand; sunisa@tsu.ac.th
[2] Research Center in Energy and Environment (RCEE), Division of Physics, Faculty of Science and Digital Innovation, Thaksin University Phatthalung, 93210, Thailand; dung_ding19@hotmail.com
[3] Research Center in Energy and Environment (RCEE), Division of Physics, Faculty of Science and Digital Innovation, Thaksin University, Phatthalung, 93210, Thailand; engr.fidaali16@gmail.com
[4] Faculty of Engineering, Thaksin University, Phatthalung, 93210, Thailand; 602995011@tsu.ac.th
[5] Université de Moncton, Edmundston (NB), Canada; yves.gagnon@umoncton.ca
[6] Research Center in Energy and Environment (RCEE), Division of Physics, Faculty of Science and Digital Innovation, Thaksin University, Phatthalung, 93210, Thailand; jompob@tsu.ac.th
* Correspondence: jompob@tsu.ac.th

Citation:
Kongprasit, S.; Chiwamongkhonkarn, S.; Ali, F.; Gagnon, Y.; Waewsak, J. Environmental impact assessment of onshore wind power plants: A case study of a 50 MW wind power plant in northeastern Thailand. *ASEAN J. Sci. Tech. Report.* **2024**, *27*(2), 39-57. https://doi.org/10.55164/ajstr.v27i2.252058

Article history:
Received: December 13, 2023
Revised: January 16, 2024
Accepted: January 26, 2024
Available online: February 29, 2024

Abstract: This research aims to assess the environmental feasibility of a wind power plant by investigating its noise disturbances, shadow flicker, and zones of visual influence. The model is applied as a case study for a 50 MW wind power plant, located in the Nakhon Ratchasima province of northeastern Thailand. The acoustic noise emissions were analyzed using the sound propagation and absorption models under the wind conditions on the site studied. The shadow flicker around each wind turbine generator, in terms of the number of hours per year, was also simulated along with the analysis of the zones of visual influence according to the number of wind turbines that can be seen by an observer from a certain distance. The results show a maximum sound level of 47 dBA, within the allowed limits of the 50 dBA legislation of the Department of Pollution Control of the Royal Thai Government. Similarly, the shadow flicker within 1 km of the wind turbines is 10 hours/year, well below the international standard of 30 hours/year. Results of the zones of visual influence indicate that between 15 and 20 turbines are visible from observation points surrounding the potential wind power plant. The results applied to this case study suggest that the potential wind power plant is well-suited regarding its environmental impacts and should typically not incur negative impacts for the local communities. Studies like these are vital to gaining the trust of the communities living near wind power plants to address their concerns and minimize opposition.

Keywords: Onshore Wind Power Plant; Noise Emission; Shadow Flicker; Zone of Visual Influence; Public Opposition.

1. Introduction

Renewable energy sources, such as solar and wind energy, are steadily replacing conventional fossil fuels as the primary source of electricity generation. Renewable energy is predicted to be the world's top electricity generation

source within three years [1]. According to a recent International Energy Agency (IEA) report on renewables, solar PV capacity will surpass gas and coal as primary energy sources by 2027. Similarly, wind generation capacity will double during this period, with offshore wind power plants contributing the bulk of the share [2]. This steady shift towards renewables is primarily due to global warming caused by greenhouse gas emissions, which led world leaders to pledge a reduction in global carbon footprint under the Paris Agreement [3]. In addition, the volatility in energy markets, notably caused by events such as the Russia-Ukraine war, has also pushed the adoption of renewables on fast tracks, especially in the European market, which heavily depends on Russian natural gas for its needs.

Thailand, an emerging economy in the ASEAN, also heavily relies on fossil fuels for its energy demands. Electricity generation is dominated by natural gas, accounting for the highest share of the Electricity Generating Authority of Thailand (EGAT), the largest producer of electricity in the country, followed by coal [4]. Thailand imports most of its natural gas and oil, with gulf gas leading the share [5], making it heavily dependent on energy imports. However, Thailand has ambitious plans to diversify its energy mix by increasing the share of renewable energy in electricity generation. Currently, renewables, including large hydropower, contribute almost 13% of the country's total electricity generation capacity [5], but the country plans to continue to increase this share.

With its power development plan (PDP 2015-2036), Thailand aims to reduce the share of fossil fuels in power generation by 30 to 40%, offsetting it by increasing the renewable energy share to 20% by 2036 [6]. Another more ambitious plan formulated by Thailand's Energy Policy and Planning Office (EPPO) aims to achieve a 50% renewable energy share to reach the carbon neutrality target by 2065 - 2070 [7]. Thailand has a total renewable electricity generation capacity of 23,856 GWh, with solar PV and wind energy contributing the highest share, 21% and 17 %, respectively. Following the global trend, both of these sources will be major contributors to the expansion of renewable energy in the country.

Thailand has an excellent onshore wind capacity that can be developed to improve the share of renewable energy in the country. Currently, the installed onshore wind capacity of Thailand reaches 1,500 MW (1.5 GW), making up 17% of the total renewable energy-based power generation in 2021 [5, 8]. However, the country has the potential to install between 13 and 17 GW of onshore wind power capacity if given the proper regulatory and policy framework [9].

Several studies have been carried out in different parts of Thailand to assess onshore wind power potential, showing encouraging results. Using the Wind Atlas Analysis and Application Program (WAsP), the wind potential assessment of Hat Yai city in Songkhla province, with its 3.5 m/s mean annual wind speed at 10 m above ground level (agl), is estimated at 2,731 MWh of wind energy generation [10]. With its mean annual wind speed of 8 m/s at 120 m agl and employing atmospheric and computational fluid dynamics (CFD) wind flow modeling, a wind power potential of 300 MW was estimated in southern Thailand [11]. In a similar study, using CFD wind flow modeling at 120 - 125 m agl, potential wind power plant sites along the Andaman coast of Thailand could generate 18 to 36 GWh/year [12]. Finally, using wind shear coefficients, the technical power potential for elevations between 65 and 120 m agl of Koh Phangan, Thailand, could reach between 10 and 20 MW [13]. These studies suggest that Thailand has good potential for developing its onshore wind energy. However, developing onshore wind power plants face challenges ranging from techno-economic aspects to socio-environment issues.

Wind turbine generators can cause noise and visual disturbances in their immediate vicinity. An international panel of experts, working under a mandate of the Government of Canada, identified through a thorough assessment of the scientific literature that the evidence is sufficient to establish a causal relationship between exposure to wind turbine noise and annoyance. At the same time, there is limited evidence to establish a causal relationship between exposure to wind turbine noise and sleep disturbances [14]. Further, the evidence suggests a lack of causality between exposure to wind turbine noise and hearing loss. In contrast, the evidence was inadequate to come to any conclusion about the presence or absence of a causal relationship between commonly claimed health impacts and exposure to wind turbine noise [14].

Nonetheless, the negative impacts of large onshore wind power plants, such as visual and noise disturbances, land use conflicts, etc., pose significant challenges to the acceptance of wind energy [15]. While large wind turbines have been well accepted in unattractive landscapes, they have faced negative social acceptance in high aesthetic quality landscapes, suggesting the visual factor is important [16]. For example, it is documented that noise and visual disturbances were considered major factors by some local community

groups in Australia opposing the development of wind energy in their area [17]. Hence, noise and visual disturbances are the primary concerns of the local communities that need to be well addressed while developing a wind power project in an area.

This study specifically focuses on assessing noise disturbances, shadow flicker, and zones of visual influence of a potential 50 MW wind power plant in the Nakhon Ratchasima province of northeastern Thailand. While the methodology of this study is independent of the location, it aims to investigate and identify the social acceptance barriers for onshore wind energy in general and specifically in Thailand.

2. Materials and Methods

2.1 Study Area

The potential wind power plant investigated is located in the Nakhon Ratchasima province of northeastern Thailand, as shown in Figure 1. The province of Nakhon Ratchasima is the most important economic hub of the northeastern region, supporting many economic activities, including tourism. Being an economic hub with a good wind resource, Nakhon Ratchasima province is home to many of Thailand's current utility-scale wind power plants, including the 90 MW KR-I wind power plant and the 103 MW first Korat wind power plant. Considering its pleasant climate, the region is also a tourist destination. The rainy season lasts almost nine months, from February to November, with September being the month with the most rain. The period of late November to early February is considered the most ideal time for tourism [18]. Thus, along with tourism, renewable energy, and notably wind energy, is vital in supporting the economic activities of this region.

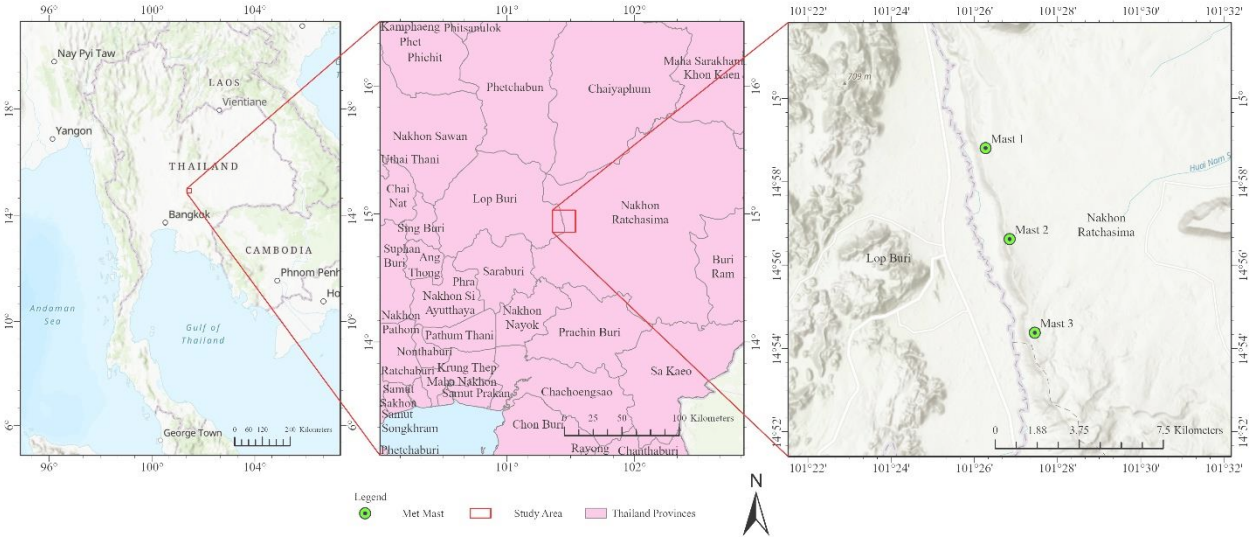

Figure 1. The study area is located in the Nakhon Ratchasima province of northeastern Thailand.

2.2 Microscale Computational Fluid Dynamics Wind Flow Modeling

The computational fluid dynamics (CFD) wind flow modeling, with a 90 m resolution, was applied for the wind speed prediction over a 10 x 10 km^2 grid, while met masts of 90 m (1 mast) and 125 m (2 masts) spread across three locations, were used to validate the numerical modeling. The positions of the three met masts are indicated in Figure 1, while their characteristics are presented in Table 1.

CFD wind flow modeling is widely used to simulate wind flow caused by the local terrain characteristics and topography and is quite helpful for developing wind energy in complex terrains [11,19]. The main inputs in CFD wind flow modeling consist of boundary conditions, i.e., terrain feature (Digital Elevation Model (DEM)) and roughness, as well as initial conditions, i.e., wind climatology in the form of wind speeds and directions at typical points of measurement in the study area. In this analysis, the ASTER Global Digital Elevation Model (GDEM) V2 provided by the USGS was used to represent the terrain feature of the

study area. The roughness was interpreted using the Land Cover Land Use (LCLU) data from the Land Development Department of Thailand [20]. The 3D DEM and roughness of the study area are presented in Figure 2.

The standard k-epsilon turbulent model was applied to execute the CFD wind flow modeling under neutral air stability conditions and air density of 1.225 kg/m^3 using the GCV solver in the WindSim simulation tool. The CFD wind flow modeling output was the spatial wind resource distribution at 137 m agl, corresponding to the hub height of the wind turbine generators used in this investigation. The distribution of the climatic wind speeds, at 90 m and 125 m agl, at the positions of the three met masts used in the CFD simulations are shown in Figure 3. This figure shows similar wind profiles for each met mast position, with average annual wind speeds of 5.81, 5.75, and 6.07 m/s, respectively, making the study area suitable for developing wind energy. Figure 4 shows the layout of the potential wind power plant and the positions of the wind turbines in the study area.

Table 1. Characteristics and period of wind measurements of the three met masts used in the study area.

Met Mast	Representative Period	Measurement Height (m agl)	Representative Period (Months)	Mean Annual Wind Speed (m/s)
KWE_Mast1	11/12/2013 (00:00) - 22/11/2016 (07:00)	125	15.0	5.81
KWE_Mast2	12/12/2013 (00:00) - 13/01/2017 (00:00)	90	14.9	5.75
KWE_Mast3	23/12/2013 (00:00) - 16/11/2016 (00:00)	125	14.9	6.07

2.3 Noise Level Measurement

One of the major barriers being faced by onshore wind power plants is their acoustic noise emissions. The acoustic footprint of large wind power plants is often the cause of concern for the residents in the vicinity, and addressing this problem is essential for the sustainable development of onshore wind energy.

The noise model of the GH WindFarmer simulation model [22] was used to model the acoustic noise emissions of the potential 50 MW wind power plant. This model designs wind power plants within the legal noise levels. The noise model calculates the attenuation for a single representative frequency and assumes hard ground surfaces.

The noise model in GH WindFarmer calculates the noise propagation at a fixed reference frequency of 500 Hz. The continuous octave-band sound pressure level at a receiver location (L_{ft}) is calculated using Eq. (1).

$$L_{\mathrm{ft}} = \mathrm{L}_W + \mathrm{D}_C - \mathrm{A} \tag{1}$$

L_W is the sound power level in dBA produced by each turbine, taking the turbine as a point source, and D_c is the directivity correction in dBA. For the case of an assumed omni-directional point sound source (i.e., a wind turbine), $D_c = 0$ dBA. The directivity of the wind turbine noise is considered when measuring the sound power level. Thus, A is the attenuation that occurs during the propagation from the point sound source to the receiver in dBA, calculated using Eq. (2).

$$\mathrm{A} = \mathrm{A}_{\mathrm{div}} + \mathrm{A}_{\mathrm{atm}} + \mathrm{A}_{\mathrm{gr}} + \mathrm{A}_{\mathrm{bar}} + \mathrm{A}_{\mathrm{misc}} + \mathrm{A}_{\mathrm{met}} \tag{2}$$

Where A_{div} is the attenuation due to geometrical divergence, A_{atm} is the attenuation due to atmospheric absorption, A_{gr} is the attenuation due to the ground effects, A_{bar} is the attenuation due to barriers, A_{misc} is the attenuation due to other effects such as foliage and areas of buildings, and A_{met} is the attenuation due to the meteorological impacts. In this investigation, there are no barriers or areas of buildings. Also, the attenuation due to the foliage of the trees is usually small. Consequently, the A_{misc} was not taken into consideration. Also, the meteorological effects are neglected since the meteorological conditions are unchanged.

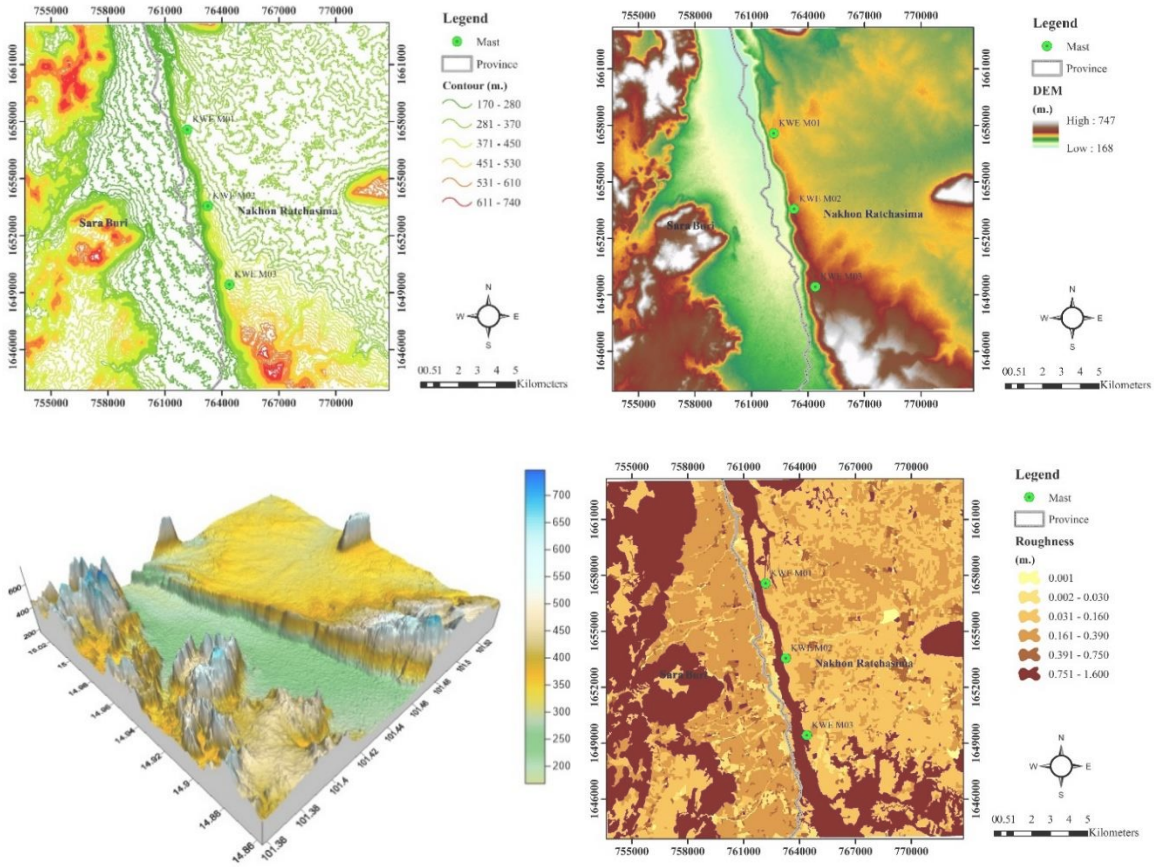

Figure 2. Contour map (upper left), 2D GDEM (upper right), 3D GDEM (lower left) and roughness (lower right) of the study area. (Source: NASA-ASTER [21])

2.3.1 Geometrical Divergence (A_{div})

The geometrical divergence attenuation $\mathbf{A}_{div}$ accounts for the spherical spreading in the free field from a point sound source over hard ground and is calculated using Eq. (3).

$$A_{div} = \left[20\log(d)+11\right]dB \tag{3}$$

Where d is the 3-dimensional distance between the source and the receiver.

2.3.2 Atmospheric Attenuation (A_{atm})

The attenuation due to atmospheric absorption $\mathbf{A}_{atm}$ is calculated using Eq. (4).

$$A_{atm} = \left[\alpha d/1000\right] \tag{4}$$

Where α is the atmospheric attenuation coefficient in dBA/km for each octave band.

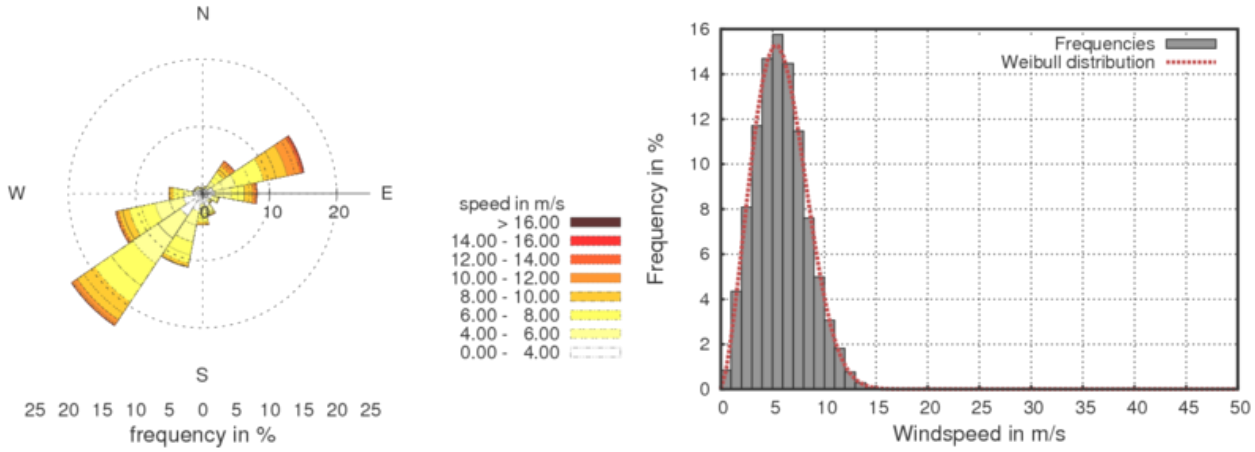

KWE Mast1, wind measurements at 125 m agl.

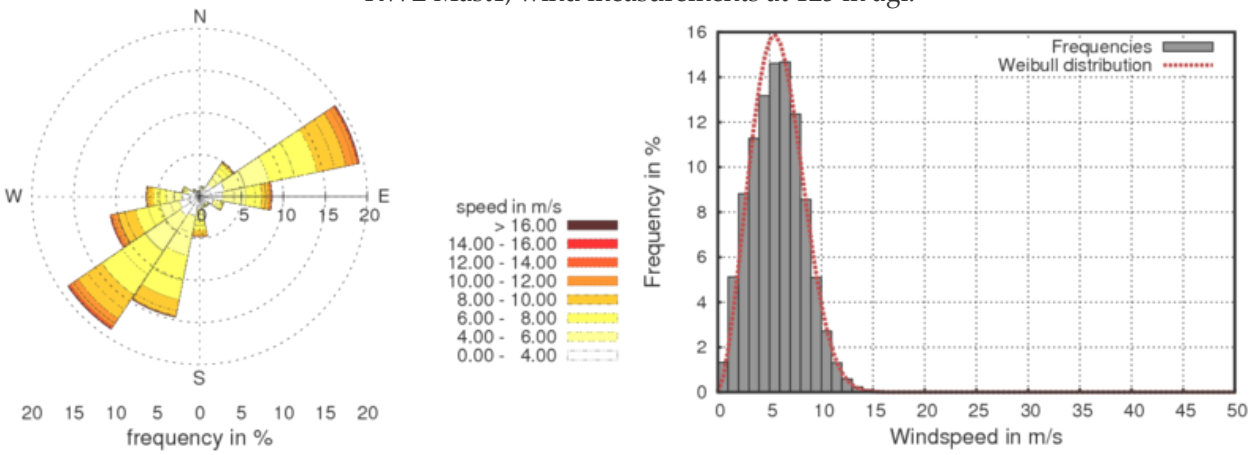

KWE Mast2, wind measurements at 90 m agl.

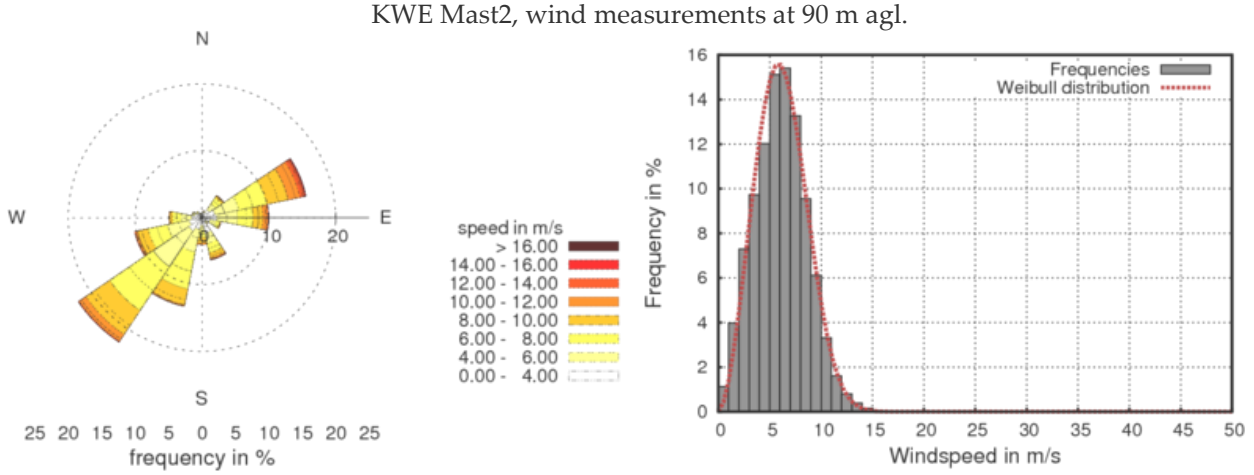

KWE Mast3, wind measurements at 125 m agl.

Figure 3. Distribution of the wind speeds, at 90 m and 125 m agl, at the positions of the met masts used in this study.

2.3.3 Ground Attenuation (A_{gr})

The total ground attenuation $\mathbf{A_{gr}}$ is the sum of the ground attenuation in the source region (A_s), the middle region (A_m), and the receiver region (A_r). In the source and receiver regions, the ground attenuation is -1.5 dB. The ground attenuation in the middle region is given by Eq. (5).

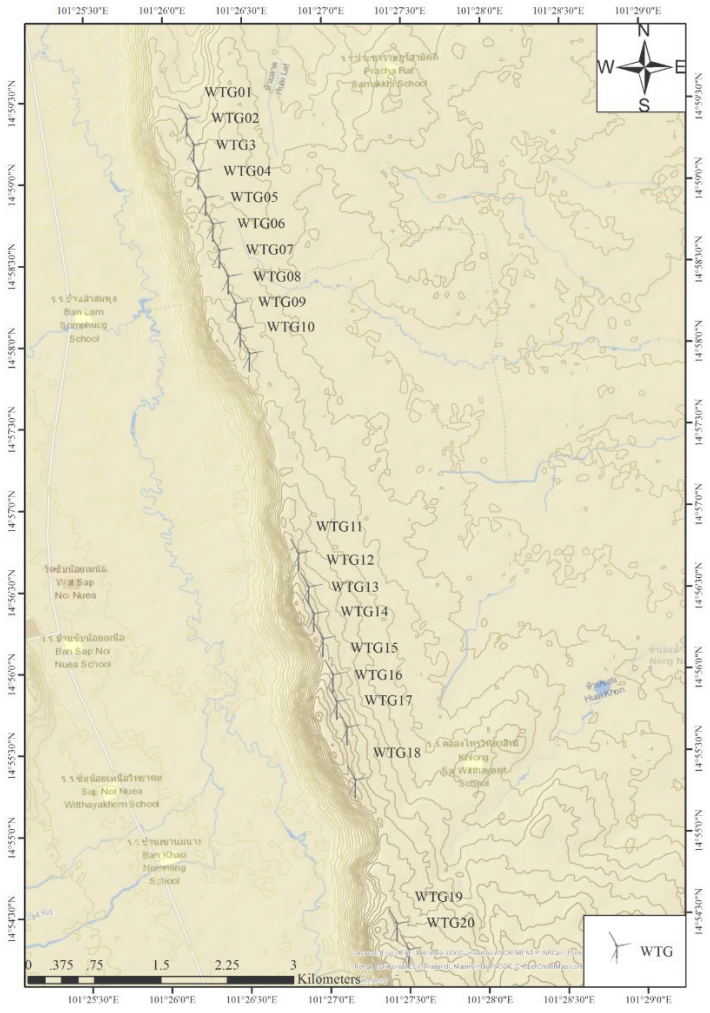

Figure 4. Layout of the potential wind power plant and the positions of the wind turbines in the study area.

$$A_m = -3qdB \tag{5}$$

$$q=\begin{cases} 1-\dfrac{30(h_s+h_r)}{dp} & \text{When } dp > 30(h_s+h_r) \\ 0 & \text{When } dp < 30(h_s+h_r) \end{cases} \tag{6}$$

Where h_s is the hub height of the wind turbine, h_r is the height of the receiver above ground, and dp is the distance from the wind turbine base to the receiver base projected onto the ground plane.

Finally, for multiple wind turbines, the combined sound pressure level for all the turbines 1 to n at a point must be calculated using Eq. (7).

$$L_{\text{total}} = 10\log\left[10^{\frac{Lft1}{10}} + 10^{\frac{Lft2}{10}} + 10^{\frac{Lft3}{10}} + \cdots + 10^{\frac{Lftn}{10}}\right] \tag{7}$$

In this work, the noise levels emitted by the 20 turbines composing the potential 50 MW wind power plant were analyzed and mapped using the above set of equations.

2.4 Shadow Flicker

The moving shadow caused by the rotation of a wind turbine rotor and blades is known as shadow flicker, and it can annoy the residents in the vicinity of a wind power plant [23]. Therefore, it is important to properly understand and address this issue to minimize the probability of opposition to wind power plant developments. The WindFarmer model [22] calculates the shadow flicker of a wind turbine using a multi-step calculation process considering many input parameters. The shadow flicker module simulates the path of the sun over one year and assesses the shadow flicker at different time intervals at multiple positions. This assessment can help turbine controllers plan the operations of the wind turbines to avoid the worst shadow flicker timing to minimize annoyance to the nearby residents.

Before the actual calculation of shadow flicker, the position of the sun at any time of the year needs to be determined. The WindFarmer model uses the following methods for determining the position of the sun [22].

2.4.1 Calculating the Hour Angle

The Hour Angle is the angular displacement of the sun, from the west or the east, of the local meridian due to the rotation of the earth on its axis at 15°/hour. To calculate the hour angle, one needs to calculate the following variables.

2.4.2 Julian Date

The Julian Date (JD) is the difference in days between the current Julian day and the Julian day at noon on January 1, 2000, and is given by Eq. (8).

$$JD = 2432916.5 + 365 \times delta + leap + day + hour/24 \tag{8}$$

Where $delta = year - 1949$, $leap = int\left[delta/4\right]$, it is defined as the integer portion of the argument.

2.4.3 Elliptic Coordinates

The elliptical coordinates are calculated using Eqs. (9 – 13).

$$n = JD - 2451545.0 \tag{9}$$

$$L = 280.460 + 0.9856474 \times n \; ; (0° \leq L < 360°) \tag{10}$$

$$g = 357.528 + 0.9856003 \times n \; ; (0° \leq g < 360°) \tag{11}$$

$$l = L + 1.915 \times \sin(g) + 0.020 \times \sin(2g) \; ; (0 \leq l < 360°) \tag{12}$$

$$ep = 23.439 - 0.0000004 \times n \tag{13}$$

Where L is the mean longitude, g is the mean anomaly, l is the ecliptic longitude, and ep is the obliquity of the ecliptic.

2.4.4 Celestial Coordinates

The celestial coordinates are the coordinates that define the position of objects in the celestial sphere or the set of numbers that pinpoint the position of objects in the sky. These coordinates are calculated by using Eq. (14 – 15).

$$\tan(ra) = \cos(ep) \times \sin(l)/\cos(l) \tag{14}$$

$$\sin(dec) = \sin(ep) \times \sin(l) \tag{15}$$

Where ra is the right ascension, and dec is the declination.

2.4.5 Greenwich Mean Sidereal Time (gmst)

The Greenwich mean sidereal time (gmst) is given by Eq. (16).

$$\text{gmst} = 6.697375 + 0.0657098242 \times \text{n} + \text{hour (UTC)} \;\; ; (0 \leq \text{gmst} < 24\text{h}) \tag{16}$$

2.4.6 Local mean sidereal time (lmst)

The local mean sidereal time (lmst) from a given gmst, the East longitude must be added to the gmst using Eq. (17).

$$\text{lmst} = \text{gmst} + \text{east. longitude} /15 \tag{17}$$

2.4.7 Hour Angle

The hour angle (ha) is calculated using Eq. (18).

$$\text{ha} = \text{lmst} - \text{ra} \; ; (-12\text{h} < \text{ha} \leq 12\text{h}) \tag{18}$$

2.4.8 Azimuth and Elevation

Finally, the sun's position definition parameters of azimuth (az) and elevation (el) are calculated using Eq. (19 – 20).

$$\sin(\text{el}) = \sin(\text{dec}) \times \sin(\text{lat}) + \cos(\text{dec}) \times \cos(\text{lat}) \times \cos(\text{ha}) \tag{19}$$

Where lat is the latitude and then the azimuth angle az can be calculated, which is measured from the north (0°):

$$\sin(\text{az}) = -\cos(\text{dec}) \times \sin(\text{ha})/\cos(\text{el}) \; ; (0° < \text{az} < 360°) \tag{20}$$

2.4.9 Occurrence of Shadow Flicker

Once the sun position and elevation are calculated, the shadow flicker is determined by the position (P) of the wind turbine, and the position of the sun (elevation angle and azimuth angle). Figure 5 illustrates the method and concept used by WindFarmer [22]. The model calculates the minimum distance from the wind turbine hub to any point (S) on the line between the sun and the point of interest (A).

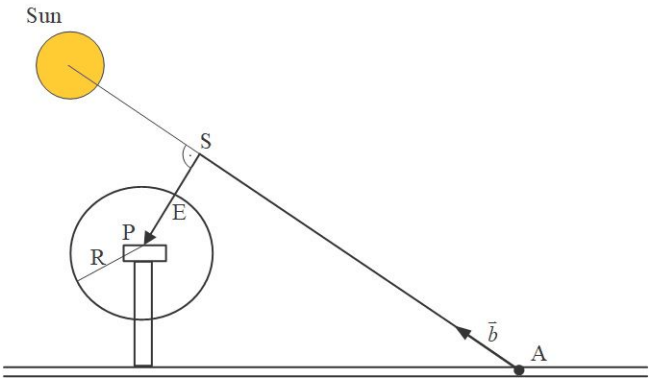

Figure 5. Conceptual model of the shadow flicker calculation in WindFarmer [22].

The points A, P, and S are represented by their vectors, $\vec{A}, \vec{P}$ and $\overrightarrow{S} = \vec{a} + \lambda_s \vec{b}$. The vector $\vec{\text{b}}$ is a unit vector pointing from the receptor to the middle of the sun and is given by Eq. (21).

$$\vec{\text{b}} = \begin{pmatrix} \cos(\text{el}) & \sin(\text{az}) \\ \cos(\text{el}) & \cos(\text{az}) \\ \sin(\text{el}) & \end{pmatrix} \tag{21}$$

For the vector AS to be perpendicular to the vector PS, we require $\vec{b} \bullet (\vec{S} - \vec{P}) = 0$. This will lead to vector SP, perpendicular to the vector AS given in Eq. (22).

$$\overrightarrow{SP} = \vec{a} + \frac{\vec{b} \bullet (\vec{P} - \vec{a})}{\vec{b}\vec{b}} \vec{b} - \vec{P} \tag{22}$$

WindFarmer compares the norm of the vector PS with the radius R of the turbine. This is repeated in time intervals of 1 minute through one year to detect if the shadow is produced at the point of analysis at each time. The model counts the minutes/day and the hours/year of shadow flicker caused by each wind turbine. The terrain features are also considered in the calculation to check for terrain features blocking the line of sight between the wind turbine and the receptor.

The rotor position is very important in the shadow flicker calculations as it is the source of the shadow. The rotor offset is calculated using Eq. (23).

$$\text{Rotor offset} = (1/2)\text{tower to diameter} + \text{tower position} + \text{disc depth} \tag{23}$$

Where tower position and disc depth are defined in the 3D Designer module of the Turbine Studio software.

Finally, employing the above shadow flicker calculation method, the shadow flicker of the wind power plant was calculated and presented for each wind turbine and all positions in the vicinity of the wind power plant.

2.5 Zones of Visual Influence (ZVI)

The zones of visual influence (ZVI) determine the visibility, suggesting the number of wind turbines that can be seen from certain distances from the wind power plant. In much research, the visual impacts of large wind turbines have been studied, and the findings show them to be directly related to the aesthetic value of the landscape. Large wind turbines in high aesthetic value areas face significant public opposition, while those in low aesthetic value areas are generally accepted quite well [25].

In this study, the ZVI assessment of the 50 MW wind power plant was also done using the WindFarmer model [22]. This model uses the line-of-sight algorithm, which checks the line of sight at regular intervals against the terrain height at each point of interest. This method offers a good degree of accuracy in comparison to other methods.

2.5.1 Standard ZVI Calculation

The standard ZVI calculates the number of wind turbines visible from the point of observer A, as shown in Figure 6, with the visibility defined as either where the hub is visible or, more sensitively, where the tip of the blade is visible.

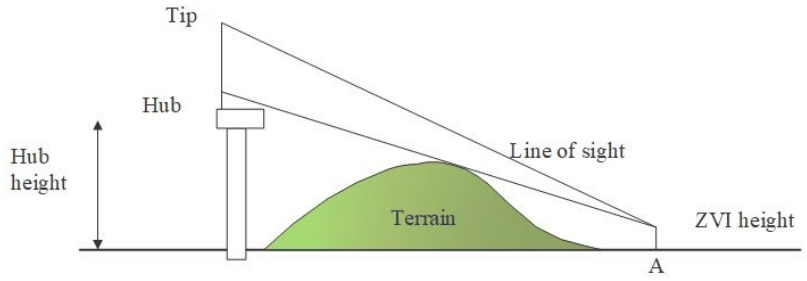

Figure 6. Standard calculation of the zones of visual influence [22].

In addition to the standard ZVI calculation, WindFarmer also calculates other ZVI parameters to assess the visual impacts of wind power plants on landscapes fully.

2.5.2 Vertical Subtended Angle

The vertical subtended angle addresses how large the wind turbines are in the observer's field of view. Wind turbines on elevated positions like hilltops will usually be visible from great distances, and the severity of the visibility declines with the distance. Figure 7 explains the vertical subtended angle calculation.

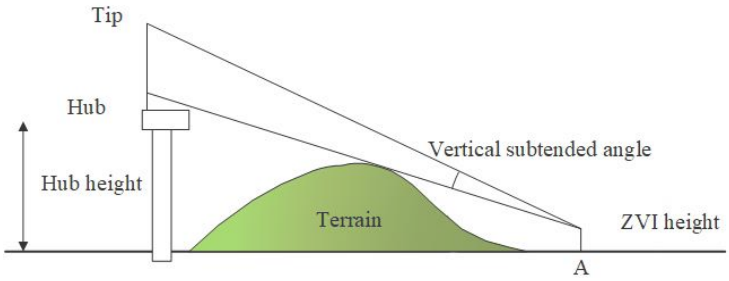

Figure 7. Conceptual representation of the vertical subtended angle [22].

2.5.3 Horizontal Subtended Angle

Similar to the vertical subtended angle, the horizontal subtended angle calculates the observer's horizontal field of view from the point of observation, as shown in Figure 8.

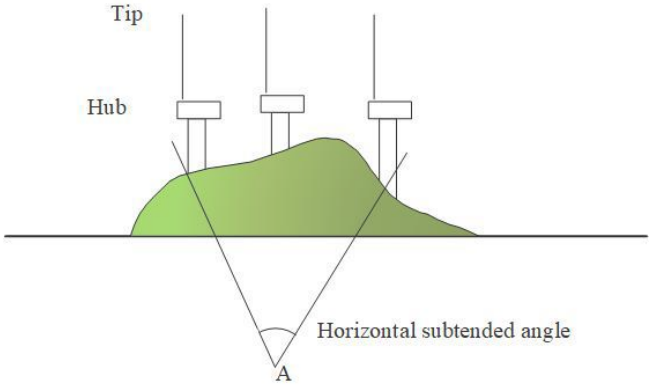

Figure 8. Conceptual representation of the horizontal subtended angle [22].

2.5.4 Visibility of the Site

Finally, using the calculations discussed above, the visibility of the site is determined. The visibility of the site determines the number of wind turbines visible from the point of observation. This work investigates and presents the number of wind turbines visible from different observation distances of the 50 MW wind power plant.

3. Results and Discussion

The microscale wind resource map at 137 m agl (10 x 10 km^2 grid, with a resolution of 90 m), including the positions of the 20 wind turbines at the location of the potential 50 MW wind power plant, is presented in Figure 9. It can be seen that the wind speeds over the study area varied in the range of 4 to 8 m/s. However, the wind speeds near the wind turbines range from 5 to 7 m/s.

This section presents and discusses the results of the noise levels, the shadow flicker, and the zones of visual influence. Many studies carried out by governments and organizations worldwide have suggested safe noise levels for wind power plant operations. In its report, the Environmental Protection Agency of Europe [24] has defined a 45 dBA or a maximum increase of 5 dBA above background noise at nearby noise-sensitive locations as allowed sound levels for normal places. Otherwise, in low-noise environments where background noise is less than 30 dBA, the allowed limit is 35 to 40 dBA.

Similarly, a report from the Energy Department of South Africa defines 35 to 40 dBA as the allowed operating sound levels for wind power plants [25]. For its part, the South Australian state government has allowed noise levels of 35 dBA for rural areas and 40 dBA for other areas, or in general, the noise level should not exceed more than 5 dBA compared to the background noise of the area [26].

In Thailand, the Department of Pollution Control has defined an acceptable noise level of 50 dBA or a noise level that is less than 10 dBA above the background noise [27]. Hence, a noise level of 35 to 50 dBA is generally allowed in various jurisdictions.

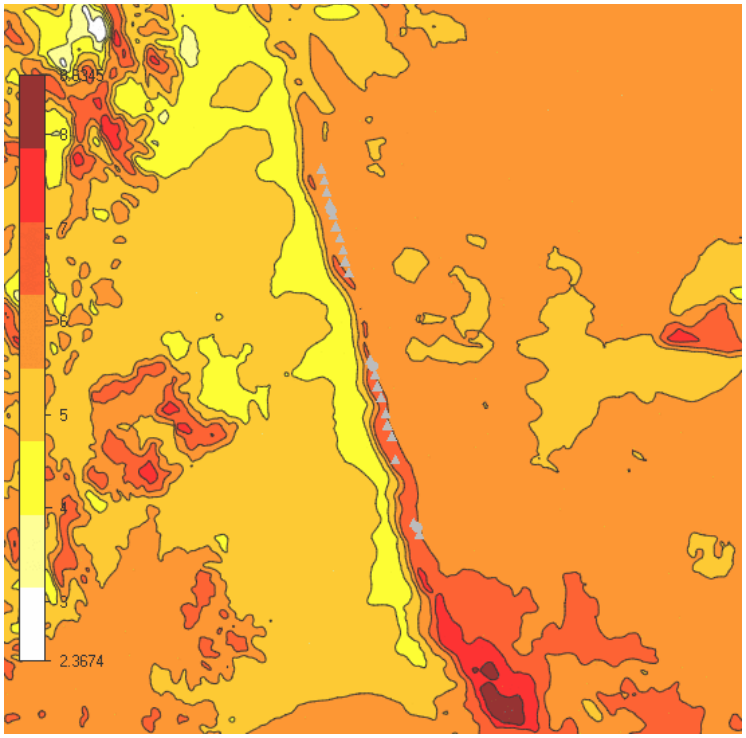

Figure 9. Microscale wind resource map at 137 m above ground level (10 x 10 km² grid, with a resolution of 90 m), including the positions of the 20 wind turbines at the location of the potential 50 MW wind power plant.

Figure 10 presents the noise emission contours for the potential 50 MW wind power plant in northeastern Thailand. It was found that the maximum noise occurred at less than 50 dBA. It can also be observed that the noise emissions are higher near each wind turbine. Thus, the noise emission levels reduce significantly with the distance of each wind turbine. This is because the noise emitted by the operation of a wind turbine under varied wind resources is attenuated by geometrical divergence, atmospheric absorption, ground effects, barriers, and other effects like foliage and areas of buildings, as well as due to the meteorological impacts.

Table 2 shows the noise produced by each wind turbine of the potential 50 MW wind power. In contrast, Table 3 illustrates the noise levels and the area affected by certain noise levels compared to the 10 x 10 km² computational grid. The wind turbines produce between 46.5 - 47.5 dBA noise levels, well below the allowed level of 50 dBA in Thailand. Apart from this, most of the area around the potential wind power plant is affected by relatively low noise levels, and only a small area of 5.9 km² (1.3% of the area studied) is in the range of 41 - 50 dBA.

Similar to the noise emission levels, the shadow flicker is another important aspect affecting the social acceptance of a wind power plant. Few countries and states have introduced legislation to limit the shadow flicker caused by wind farms. Governments in Australia, England, Ireland, and many other countries require that the shadow flicker of wind power plants be below 30 hours/year and 30 minutes/day [28, 29]. So far, Thailand has not introduced any specific legislation for shadow flickering of wind power plants. Table 2 also shows the shadow flicker of each wind turbine on an annual basis. In contrast, Table 4 shows the area affected by the shadow flicker of the potential wind power plant in comparison to the 10 x 10 km² computational grid. While the majority of the area studied has no shadow flicker (73.7% of the area studied) or less than 10 hours per year (11.9% of the area studied), shadow flicker of an individual wind turbine is in the range of 50 hours/year for nearly 10% of the area studied. Less than 2% of the area studied has shadow flicker above 100 hours per year. Figure 11 summarizes the shadow flicker in graphical form, confirming that the shadow flicker for all wind turbines is well within the 1000 m buffer zones established for each wind turbine. Thus, the shadow flicker should have limited impacts on the population.

Finally, the visual impact of wind energy developments is highly related to the quality of the landscape and the perception of the residents living around it. Wind energy developments face opposition in

high-value aesthetic landscapes and are well-accepted in areas with lower aesthetic values. Similarly, some people feel annoyed due to the wind turbines obstructing the field of view, while others consider it a positive addition to the landscape. Table 2 provides the zone of visual influence for each wind turbine, while Figure 12 shows different areas with the number of wind turbines visible. Generally, between 15 and 20 turbines are visible from observation points surrounding the potential wind power plant.

Table 2. Noise emission levels, shadow flicker, and zones of visual influence of the potential 50 MW wind power plant.

Turbine	Noise (dBA)	Shadow Flicker (hours/year)	Zone of Visual Influence (Turbine)
WTG 1	47.10	102.4	17
WTG 2	47.57	87.4	15
WTG 3	47.69	78.4	20
WTG 4	47.72	93.9	20
WTG 5	47.73	140.0	20
WTG 6	47.72	88.8	20
WTG 7	47.68	83.0	20
WTG 8	47.70	133.8	20
WTG 9	47.66	71.8	20
WTG 10	47.12	62.5	20
WTG 11	46.81	60.0	12
WTG 12	47.35	85.0	20
WTG 13	47.60	116.0	20
WTG 14	47.42	95.8	15
WTG 15	47.41	124.5	20
WTG 16	47.52	136.3	20
WTG 17	47.18	98.9	20
WTG 18	46.50	74.9	10
WTG 19	46.79	50.8	20
WTG 20	46.82	85.7	20

Table 3. The area is affected by the noise emissions of the potential 50 MW wind power plant compared to the 10 x 10 km^2 computational grid.

Noise (dB(A)	Area (km^2)	%
> 0	17.66	4.4
1.0 - 10.0	131.24	32.8
11.0 - 20.0	150.22	37.6
22.0 - 30.0	69.91	17.5
31.0 - 40.0	25.80	6.5
41.0 - 50.0	5.89	1.3

Table 4. The area affected by shadow flicker of the potential 50 MW wind power plant.

Shadow Flicker (hours/year)	Area (km^2)	%	Cumulative (%)
No shadow flicker	73.7	73.7	73.7
0.1 - 10	11.9	11.9	85.6
10.1 - 100	9.7	9.7	95.3
100.1 - 200	2.8	2.8	98.1
200.1 - 300	1.1	1.1	99.2
300.1 - 400	0.5	0.5	99.7
400.1 - 500	0.3	0.3	100
500.1 - 600	0.02	0.02	100
Total Area	**26.3**	**100.0**	**100**

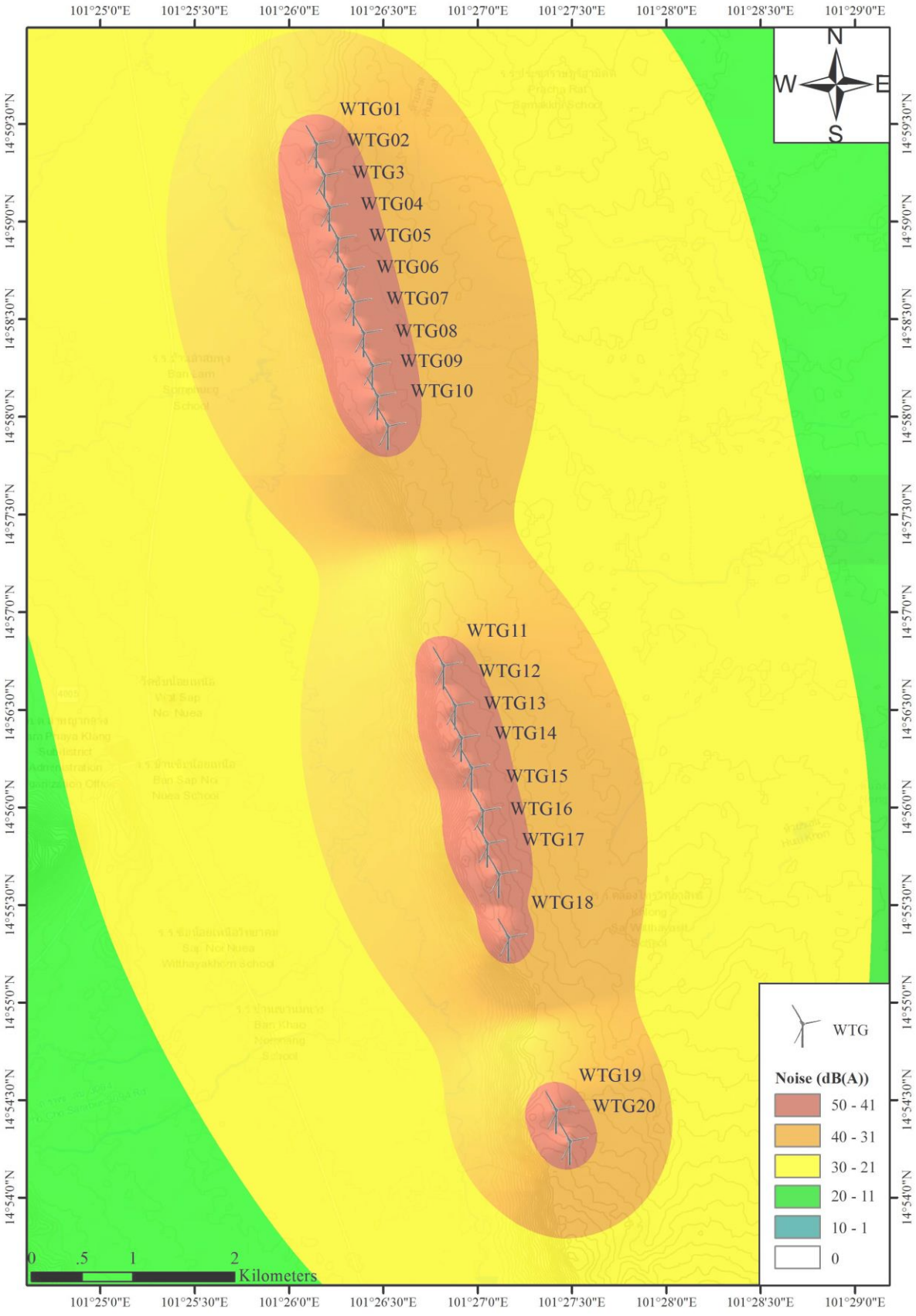

Figure 10. Noise emission contours of the 20 wind turbines composing the potential 50 MW wind power plant.

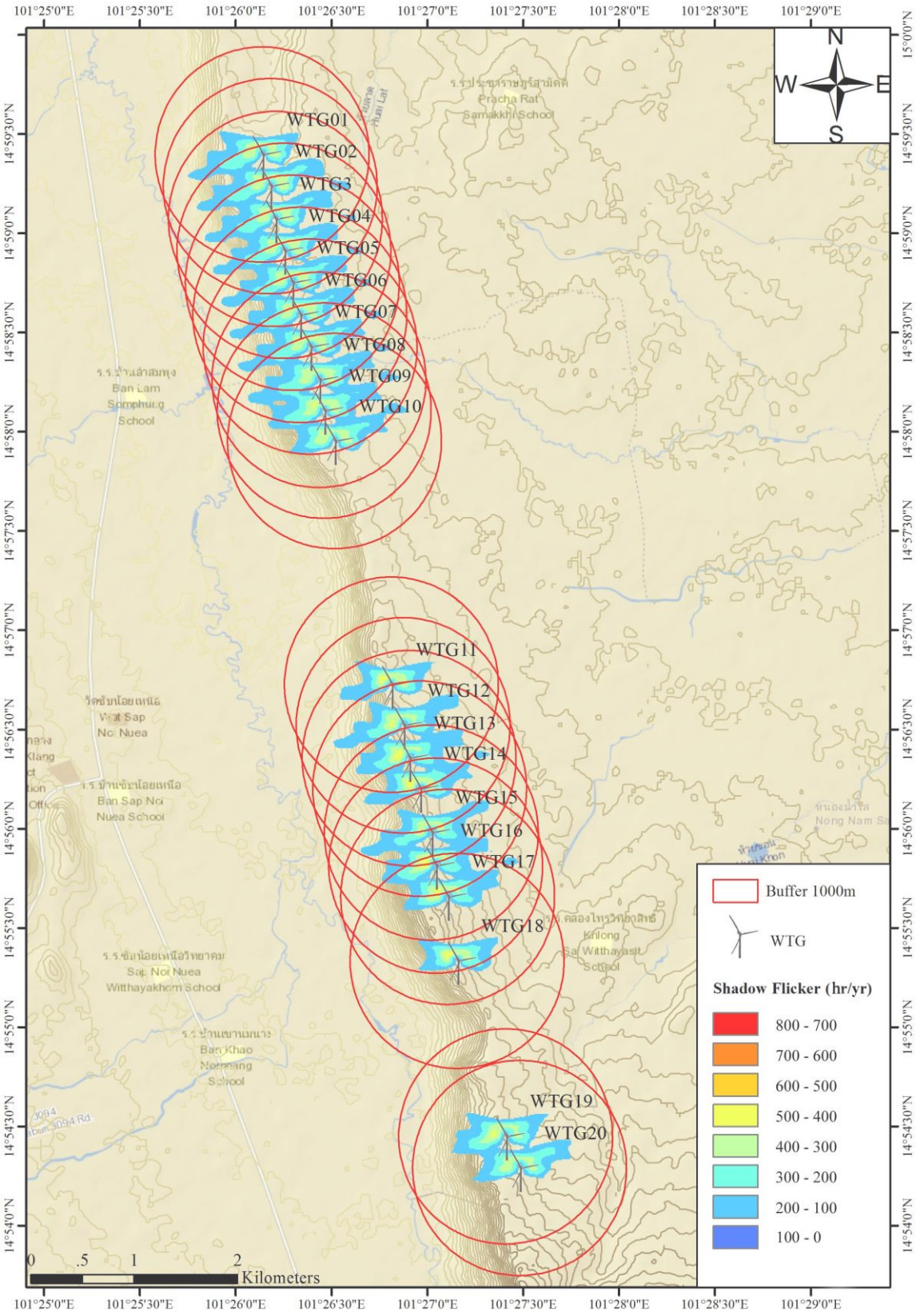

Figure 11. Shadow flicker of the potential 50 MW wind power plant.

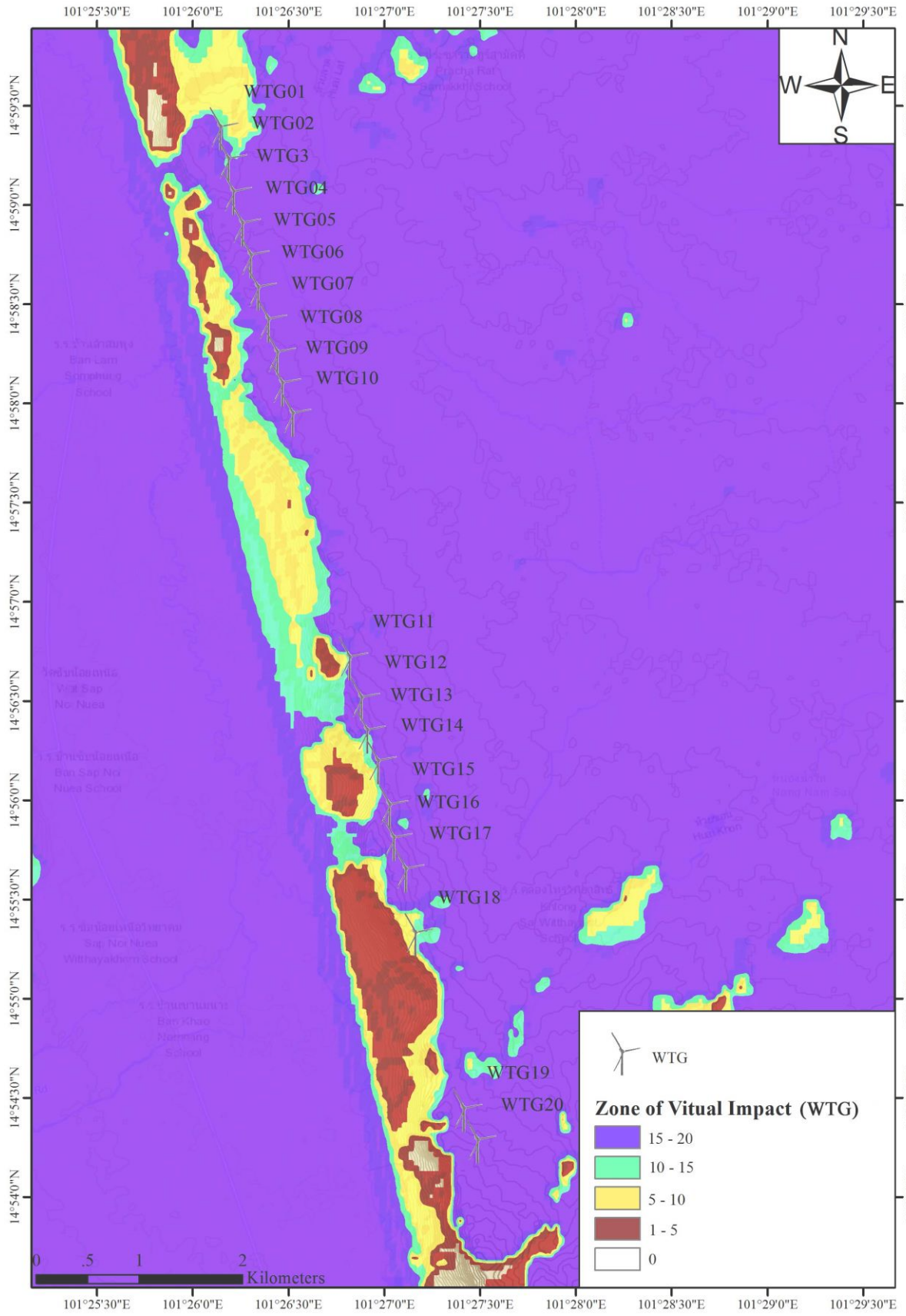

Figure 12. Zone of visual influence of the potential 50 MW wind power plant.

4. Conclusions

Onshore wind power plants are important renewable energy sources and will be crucial for countries like Thailand to transition to green, non-GHG-emitting energy. But despite being the most popular renewable energy source, onshore wind power plants are susceptible to public opposition due to their environmental impacts. Onshore wind power plants face acceptance issues due to noise and shadow flicker disturbances they cause in their vicinity. In addition, their visual impacts are also considered undesirable, especially in highly aesthetic-valued areas where it is believed to have a profound effect on the land value. Therefore, it is vital to fully understand and address these issues while developing a wind power plant in an area to avoid conflicts and develop wind resources sustainably. This research aimed to assess the noise emission levels, the shadow flicker, and the visual impacts of a potential 50 MW wind power plant located in the Nakhon Ratchasima province of northeastern Thailand.

The WindFarmer simulation model [22] assessed the noise emission levels, the shadow flicker, and the zones of visual influence of the wind power plant. With noise levels of 46.5 to 47.5 dBA, the wind power plant would be well within the allowable range of 50 dBA. Similarly, it also has a good shadow flicker profile of less than 10 hours/year for most of the area surrounding the site, way below the value of 30 hours/year seen in other jurisdictions. Finally, the results of the zones of visual influences indicate that between 15 and 20 wind turbines are visible from observation points surrounding the potential wind power plant. The results applied to this case study suggest that the potential wind power plant is well-suited regarding its environmental impacts and should typically not incur negative impacts for the local communities. Studies like these are vital to gaining the trust of the communities living near wind power plants to address their concerns and minimize opposition.

On a broader scale, the method used in this study can be employed in any other part of the world to assess and better plan the development and installation of onshore wind power plants. Beyond the technical, economic, and environmental aspects of wind power plants, future investigations should look at the impacts of wind turbines and wind power plants on biodiversity and the social acceptance of wind power plants. Understanding these issues better should identify mitigation strategies in wind energy development as an important component of the energy transition.

5. Acknowledgements

The authors would like to thank the Research and Development Institute and the Research Center in Energy and Environment (RCEE) of Thaksin University for their financial support of this work under the framework of an International Collaborative Research Project.

Author Contributions: Conceptualization, K.S. and W.J.; methodology, K.S.; software, C.S.; validation, K.S.; formal analysis, M.P.; investigation, K.S. and W.J.; writing-original draft preparation, K.S.; writing-review and editing, A.F. and G.Y.; visualization, W.J.; supervision, W.J. and G.Y.; All authors have read and agreed to the published version of the manuscript.

Funding: The authors thank the private company for their financial support and the data used in this work. The private company was not involved in the research work or in preparing and submitting this publication.

Conflicts of Interest: There is no conflict of interest.

References

[1] International Energy Agency (IEA). *Electricity Market Report 2023*. **2023**. https://www.iea.org/reports/electricity-market-report-2023. (accessed April 25, 2023)

[2] International Energy Agency (IEA). *Renewables 2022: Analysis and Forecast to 2027*. **2022**. https://www.iea.org/reports/renewables-2022 (accessed May 2, 2023).

[3] United Nations Framework Convention on Climate Change (UNFCCC). *Adoption of the Paris Agreement - Paris Agreement Text English*, 2015. https://unfccc.int/sites/default/files/english_paris_agreement.pdf. (accessed May 1, 2023).

[4] Electricity Generating Authority of Thailand (EGAT). *Annual Report 2021 Electricity Generating Authority of Thailand*. **2022**. https://www.egat.co.th/home/en/wp-content/uploads/2022/06/EGAT-Annual-2021-EN_2022-06-22.pdf. (accessed May 3, 2023).
[5] Energy Regulatory Commission (ERC). *Annual Report - Energy Regulatory Commission of Thailand*. **2021**. https://www.erc.or.th/en/annual-report/3749 (accessed May 3, 2023).
[6] Energy Policy and Planning Office (EPPO). *Thailand Power Development Plan (2015-2036)*. **2015**. https://www.eppo.go.th/images/POLICY/ENG/PDP2015_Eng.pdf. (accessed April 25, 2023).
[7] Energy Policy and Planning Office (EPPO). *Meeting Resolution on Energy Saving Methods No. 2/2021 (No. 154*). **2021**. https://www.eppo.go.th/index.php/th/component/k2/item/17213-nepc-prayut04-08-64. (accessed April 30, 2023).
[8] International Renewable Energy Agency (IRENA). *Renewable Energy Outlook – Thailand*. **2017**. https://www.irena.org//media/Files/IRENA/Agency/Publication/2017/Nov/IRENA_Outlook_Thailand_2017.pdf (accessed April 10, 2023).
[9] Global Wind Energy Council (GWEC). *An Industry Perspective on Strengthening Onshore Wind Development in Thailand. **2019***. https://ec.europa.eu/eurostat/statistics- (accessed April 29, 2023).
[10] Kamdar, I.; Taweekun, J. Assessment of Wind Energy Potential of Hat Yai (Songkhla), Thailand. *IOP Conference Series: Materials Science and Engineering*. **2021**, *1163*(1), 012001. https://doi.org/10.1088/1757-899X/1163/1/012001
[11] Waewsak, J.; Chancham, C.; Chiwamongkhonkarn, S.; Gagnon, Y. Wind Resource Assessment of the Southernmost Region of Thailand Using Atmospheric and Computational Fluid Dynamics Wind Flow Modeling. *Energies*. **2019**, *12*, 1899. https://doi.org/10.3390/EN12101899.
[12] Niyomtham, L.; Lertsathittanakorn, C.; Waewsak, J.; Gagnon, Y. Mesoscale/Microscale and CFD Modeling for Wind Resource Assessment: Application to the Andaman Coast of Southern Thailand. *Energies*. **2022**, 15, 3025. https://doi.org/10.3390/EN15093025.
[13] Werapun, W.; Tirawanichakul, Y.; Waewsak, J. Wind Shear Coefficients and their Effect on Energy Production. *Energy Procedia*. **2017**, 138, 1061-1066. https://doi.org/10.1016/J.EGYPRO.2017.10.111.
[14] Council of Canadian Academes, 2015. "Understanding the Evidence: Wind Turbine Noise". Ottawa (ON), Canada: The Expert Panel on Wind Turbine Noise and Human Health, Council of Canadian Academes, 180 p. (Experts Panel (alphabetical order): H.W Davies, Y. Gagnon, C. Giguère, T.L. Guidotti (Chair), S. Grace, R.V. Harrison, B. Howe, D.A. Johnson, K. Persson Waye, J.D. Roberts). https://cca-reports.ca/reports/understanding-the-evidence-wind-turbine-noise/ (accessed April 29, 2023).
[15] Huber, S.; Horbaty, R.; Ellis, G. *Social Acceptance of Wind Power Projects: Learning from Trans-National Experience*, 5th ed.; Palgrave Macmillan UK: London, England. **2012**, 215-278. https://doi.org/10.1057/9781137265272_11
[16] Molnarova, K.; Sklenicka, P.; Stiborek, J.; Svobodova, K.; Salek, M.; Brabec, E. Visual Preferences for Wind Turbines: Location, Numbers and Respondent Characteristics. *Applied Energy*. **2012**, *92*, 269–278. https://doi.org/10.1016/j.apenergy.2011.11.001.
[17] Hall, N.; Ashworth, P.; Devine-Wright. P. Societal Acceptance of Wind Farms: Analysis of Four Common Themes across Australian Case Studies. *Energy Policy*. **2013**, *58*, 200–208. https://doi.org/10.1016/j.enpol.2013.03.009.
[18] Weather Spark. *Nakhon Ratchasima Climate, Weather by Month, Average Temperature (Thailand)*.https://weatherspark.com/y/114253/Average-Weather-in-Nakhon-Ratchasima-Thailand-Year-Round (accessed May 1, 2023).
[19] Niyomtham, L.; Waewsak, J.; Kongruang, C.; Chiwamongkhonkarn, S.; Chancham, C.; Gagnon, Y. Wind Power Generation and Appropriate Feed-in-Tariff under Limited Wind Resource in Central Thailand. *Energy Reports*. **2022**, *8*, 6220–6233. https:// doi.org /10. 1016/j.egyr.2022.04.068.
[20] https://lddcatalog.ldd.go.th/dataset/ldd_21_01 (accessed December, 11 2022).
[21] https://asterweb.jpl.nasa.gov/gdem.asp (accessed December, 11 2022).
[22] GH and Partners. *GH WindFarmer: Theory Manual*. http://www.ccpo.odu.edu/~ klinck/Reprints/PDF/garradhassan2009.pdf. (accessed May 10, 2023).
[23] Haac, R.; Darlow, R.; Kaliski, K.; Rand, J.; Hoen, B. In the Shadow of Wind Energy: Predicting Community Exposure and Annoyance to Wind Turbine Shadow Flicker in the United States. *Energy Research & Social Science*. **2022**, *87*, 102471. https://doi.org/10.1016 /j. er ss.2021.102471.

[24] Environmental Protection Agency Office of Environmental Enforcement (OEE). *Guidance Note on Noise Assessment of Wind Turbine Operations at EPA Licensed Sites (NG3)*. **2011**. https://www.epa.ie /publications/monitoring--assessment/noise/Wind_Turbine_web.pdf. (accessed May 11, 2023).
[25] Powered by Wind. *Noise Levels of Wind Farms*, 2018. http://www.poweredbywind. co.za/dl/english/fact sheet5.pdf. (accessed May 5, 2023).
[26] Corke, T.; Nelson, R. *Wind Farms Environmental Noise Guidelines*. **2018**. https:// doi.org/10.1201/b22301-8. (accessed May 8, 2023).
[27] Waewsak, J.; Kongruang, C.; Gagnon, Y. Assessment of Wind Power Plants with Limited Wind Resources in Developing Countries: Application to Ko Yai in Southern Thailand. *Sustainable Energy Technologies and Assessments*. **2017**, *19*, 79-93. https:// doi.org/ 10.1016/ j.seta.2016.12.001.
[28] Poli, S. *Annex D Shadow Flicker Assessment Cañadon Leon Windfarm*. **2019**. https://www3.dfc.gov/Environment/EIA/canadon/ Supp_ ESIA_ANNEX_D.pdf. (accessed May 10, 2023)
[29] Brinckerhof, P. *Update of UK Shadow Flicker Evidence Base*. **2011**. https://assets.publishing.service.gov.uk/government/uploads/system/uploads/attachment_data/file/48 052/1416-update-uk-shadow-flicker-evidence-base.pdf. (accessed May 12, 2023).